# MODELING JP-8 FUEL EFFECTS ON DIESEL COMBUSTION SYSTEMS

Peter Schihl*, Laura Hoogterp, Harold Pangilinan, Ernest Schwarz, Walter Bryzik
RDECOM-TARDEC
Warren, MI. 48397-5000

## ABSTRACT

The U.S. Army currently utilizes Jet Propulsion 8 (JP-8) and Diesel Fuel number 2 (DF-2) as the two prime fuels for ground mobility applications. These two fuels have significant physicochemical property differences (such as density, distillation curve, and cetane number) that may result in fuel-affected varying combustion behavior in diesel engines under various operating conditions. Since engine manufacturers rely solely on DF-2 for commercial vehicle applications most domestic industry, university, and national laboratory lead diesel engine combustion system research activities have not encompassed JP fuels. Instead, much effort has been spent exploring DF-2 evaporation behavior, pre-ignition kinetics, high pressure spray formation and subsequent energy release processes, particulate matter formation and oxidation, and nitrous oxide formation pathways under diesel relevant pressures and temperatures. To date, there is little information published in the literature on the topic of JP-8 spray combustion though some activities have recently begun to address specific sub-processes including low temperature chemistry, ignition chemistry, and turbulent flame speed, but at thermodynamic conditions near the lower end of typical diesel combustion conditions.

The intent of this submission is to address a portion of this JP-8 technical 'gap' by developing a methodology for determining the evaporation rate of JP-8 in a direct-injection diesel engine and extrapolate this key combustion affecting process to predict energy release rate profiles and subsequent cylinder pressure rise rate in a current military diesel engine through extrapolation of the current knowledge base for heavy hydrocarbon ignition toward a medium worst case cetane number scenario. Furthermore, the extrapolated JP-8 ignition cases will be compared with recent constant volume data taken under a limited range of charge densities and temperatures to substantiate the initial JP-8 ignition behavior extrapolation.

## INTRODUCTION

The 'one fuel forward' policy was initiated through DOD Directive 4140.43 as a means to reduce a portion of the logistics burden associated with bringing multiple fuels to the battlefield. Almost twenty years ago a representative sample of Army diesel engines were selected for a series of durability tests that included DF-2 at standard conditions, Jet A at standard conditions, and Jet A at elevated fuel temperature (Miklos, 1989) in order to benchmark use of JP-8 in Army ground vehicles. These series of tests revealed that the selected diesel engines exhibited a rated speed power loss ranging from 2% to 10% at standard conditions and 4% to 25% at elevated fuel temperatures. Furthermore, three out of the five engines exhibited fuel system reliability issues that were subsequently resolved to allow for JP-8 use in the field. The power loss issue is related to both the lower energy per unit volume and combustion differences associated with JP-8 versus DF-2 especially considering diesel injection systems tend to volumetrically meter the engine fuel flow rate. Such losses are unavoidable since such engines are commercial products whose calibration strategies are based on DF-2 under the guise of meeting U.S. Environmental Protection Agency (EPA) emission standards. This latter constraint is normally alleviated for combat vehicle applications that are allotted a National Security Exemption (NSE) under the Code of Federal Regulations (CRF) 40. To date, most tactical vehicles employ commercial engines and thus tend to meet a past EPA emissions standard based on the original production date of the engine in question but in the future it will be very difficult to both integrate such engine systems into existing tactical vehicles and also operate on JP-8 without significant vehicle performance issues.

One particular engine included within the aforementioned sample set of five exhibited an extreme loss of power that resulted in a necessary required physical change to the fuel pump delivery rate based on fuel type. This engine was eventually re-rated to a much higher power level that resulted in additional combustion system issues that could lead to engine failure that revolved around the spray targeting and engine calibration strategies – this engine is the focus of this study. Other military engines have exhibited less dramatic effects of operating on JP-8 under high temperature conditions such as up to a few hundred revolution per minute (RPM) change in peak torque speed (private communication with TARDEC propulsion laboratory) while still other engines have demonstrated an insignificant rated speed power change while operating on JP-8 at standard and elevated operating temperatures (private communication with TARDEC propulsion laboratory).

# Report Documentation Page

*Form Approved*
*OMB No. 0704-0188*



| 1. REPORT DATE | 2. REPORT TYPE | 3. DATES COVERED |
|---|---|---|
| **24 SEP 2006** | **N/A** | |

| 4. TITLE AND SUBTITLE | 5a. CONTRACT NUMBER |
|---|---|
| **Modeling JP-8 Fuel Effects on Diesel Combustion Systems** | 5b. GRANT NUMBER |
| | 5c. PROGRAM ELEMENT NUMBER |
| 6. AUTHOR(S) | 5d. PROJECT NUMBER |
| **; ; ; ; Schihl /PeterHoogterp /LauraPangilinan /HaroldSchwartz /ErnestBryzik /Walter** | 5e. TASK NUMBER |
| | 5f. WORK UNIT NUMBER |
| 7. PERFORMING ORGANIZATION NAME(S) AND ADDRESS(ES) | 8. PERFORMING ORGANIZATION REPORT NUMBER |
| **REDCOM - TARDEC 6501 E 11 Mile Rd Warren, MI 48397-5008** | **16303** |
| 9. SPONSORING/MONITORING AGENCY NAME(S) AND ADDRESS(ES) | 10. SPONSOR/MONITOR'S ACRONYM(S) |
| | 11. SPONSOR/MONITOR'S REPORT NUMBER(S) |

12. DISTRIBUTION/AVAILABILITY STATEMENT
**Approved for public release, distribution unlimited.**

13. SUPPLEMENTARY NOTES

14. ABSTRACT

15. SUBJECT TERMS

| 16. SECURITY CLASSIFICATION OF: | | | 17. LIMITATION OF ABSTRACT | 18. NUMBER OF PAGES | 19a. NAME OF RESPONSIBLE PERSON |
|---|---|---|---|---|---|
| a. REPORT | b. ABSTRACT | c. THIS PAGE | | | |
| **unclassified** | **unclassified** | **unclassified** | **SAR** | **8** | |

It is anticipated that future commercial diesel engines will become even more sensitive to fuel type given the necessary combustion system strategies that will be utilized to meet the EPA 2010 heavy-duty diesel engine emission standards. Such strategies include use of sophisticated, sulfur sensitive aftertreatment devices and variants of homogeneous charge compression ignition (HCCI) and premixed charge compression ignition (PCCI) that essentially are a distributed bulk energy release approach that lead to high pressure rise rates dependent on fuel ignition chemistry. Without closed loop control through utilization of an in-cylinder pressure sensor in each cylinder, it will be almost impossible to operate such engines on fuels with varying ignition properties.

With the various aforementioned challenges associated with integrating commercial diesel engines into military applications it is paramount the research community continues to study important combustion affecting differences between JP-8 and DF-2 including evaporation rate variances, low temperature chemistry, pre-ignition chemistry, bulk spray formation, and fuel system delivery rate variances to name a few key areas of study. Some work has begun on low temperature chemistry (Cernansky, 2006), bulk pre-ignition behavior (Hanson, 2006), and also on spray flame spread rate (Metghalchi, 2006), but not at boundary conditions that cover ranges experienced by a typical diesel engine. In particular, diesel engines typically exhibit bulk combustion chamber temperatures and pressures at start of injection in the ranges of 800 K to 1100 K and 30 bar to 110 bar. The aforementioned JP-8 ignition study was conducted in a shock tube and limited to 30 bar but with temperatures up to 1200 K (Hanson, 2006) while the turbulent flame speed study was conducted in a constant volume bomb and limited to 10 bar and approximately 800 K (Metghalchi, 2006). Though both studies are important initial attempts at addressing JP-8 combustion subprocesses behavior, much effort still needs to be spent acquiring relevant measurements more indicative of real world cylinder pressure and temperature since the ignition delay period in an engine is highly dependent on these key thermodynamic parameters and also the local air-fuel ratio.

This submission will directly address such variances in evaporation rate, the bulk (mean) pre-ignition chemistry, i.e. ignition delay period, and bulk features of the spray formation process.

## 1. EVAPORATION RATE MODELING

The evaporation process in a diesel jet under the constraint that ignition occurs during the injection event can be modeled as a steady-state jet whose evaporation rate is mixing controlled under the assumption of a finely atomized spray with an advantageous surface area to volume ratio promoting a saturated state at the bulk break-up length of the jet (Siebers, 1999). Additionally, this model is based on the judicious selection of a single pure hydrocarbon fuel surrogate that is deemed to properly simulate the real world fuel's evaporation characteristics. For completeness, the model is given below and is based on applying the conservation of mass, momentum, and energy to a rectangular control volume that encompasses a propagating conical fuel jet whose tip has reached the saturated state condition:

$$L_b = \frac{b}{a}\sqrt{\frac{\rho_f}{\rho_a}}\,\frac{\sqrt{C_a}\bullet d}{\tan(\frac{\theta}{2})}\sqrt{\left(\frac{2}{B_s}+1\right)^2-1} \qquad \textbf{(1)}$$

where a and b are constants, $\rho_f$ is the liquid fuel density, $\rho_a$ is the ambient density, $C_a$ is the nozzle area coefficient, $\theta$ is the spray formation angle, d is the orifice diameter, and $B_s$ is the fuel to ambient gas flow rate ratio or evaporation coefficient. Furthermore, this latter constant $B_s$ is fuel dependent and based on the iterative solution of the conservation of mass and energy. For completeness this relationship is shown below:

$$B_s = \frac{Z_a(T_a,P_a-P_s)\bullet P_a \bullet M_f}{Z_f(T_s,P_s)\bullet(P_a-P_s)\bullet M_a} = \frac{h_a(T_a,P_a)-h_a(T_s,P_a-P_s)}{h_f(T_s)-h_f(T_f,P_a)} \qquad \textbf{(2)}$$

where $Z_a$ and $Z_f$ are the ambient and fuel vapor compressibility, $T_f$ is the injected liquid fuel temperature, $T_a$ and $P_a$ are the ambient temperature and pressure, $M_f$ and $M_a$ are the fuel and ambient molecular weights, $T_s$ and $P_s$ are the fuel saturation temperature and pressure, $h_a$ is the ambient enthalpy, and $h_f$ is the fuel enthalpy.

This modeling approach exhibited very good agreement with experimental data acquired for a variety of heavy-hydrocarbon fuels under thermodynamic conditions experienced in a diesel engine under 'warmed up' conditions through comprehensive constant volume bomb experiments, i.e. this assumption is not valid for cold start or light load under extremely cold ambient conditions (Siebers 1998, 1999). The model was compared to data collected for commercial grade DF-2, heptamethylnonane (HMN), and cetane, and furthermore compared with possible single component hydrocarbon surrogates that both best represent the 90% distillation point of the particular given fuel and also have readily available thermodynamic properties that cover the proper temperature and pressure ranges. During this study it was discovered that either cetane or heptadecane were acceptable surrogates for simulating the evaporation rate of DF-2 under diesel spray type thermodynamic conditions since either surrogate has a boiling point near

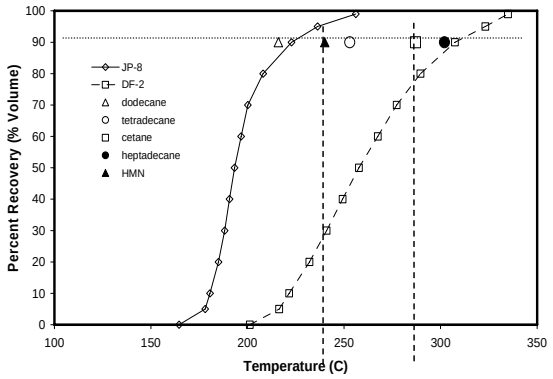


**Figure 1: DF-2 and JP-8 Distillation Curves.**

the 90% distillation point of DF-2. Such an approach maybe extrapolated to other fuels including JP-8, but with careful consideration given to using a multi-component surrogate. Therefore, a threefold approach will be used to develop a methodology for using multi-component surrogates: (1) potential surrogate subcomponents will be selected as candidates for fuels with current experimental evaporation rate databases; (2) a method of properly determining fuel properties for multi-component surrogates will be developed and benchmarked against various fuels; (3) a surrogate will be chosen based on (1) and (2) that best represents JP-8.

### 1.1 Surrogates and Thermodynamic Properties

A close look at representative distillation properties of JP-8 and HMN reveals the possibility of three surrogate subcomponents – dodecane, tetradecane, and cetane – see table 1 and figure 1. Each of these three possible subcomponents cover the necessary boiling point range of JP-8, HMN, and DF-2 and also either have published thermodynamic property relationships or derived property sets (American Petroleum Institute, 1997). In particular, the saturation pressure and liquid density relationships were published for each of these pure hydrocarbon fuels while the compressibility and enthalpy relationships were developed through accurate, piece-wise curve-fits based on given property values (American Petroleum Institute 1997; Moran and Shapiro, 2000). These resulting relationships were benchmarked for accuracy using equations (1) and (2) against predictions previously made by Sandia National Laboratory (Siebers, 1999; Schihl et al., 2006) for both cetane and DF-2. Furthermore, these relationships were also compared through equations (1) and (2) against dodecane data collected from a variety sources (Verhoeven et al., 1998; Schmalzing et al., 1999, Kim et al., 2002) and showed a reasonable level of predictive capability – see figure 2.

Thus, the following thermodynamic relationships are valid for the three surrogate subcomponents and maybe used for evaporation modeling or other types of thermodynamic modeling efforts.

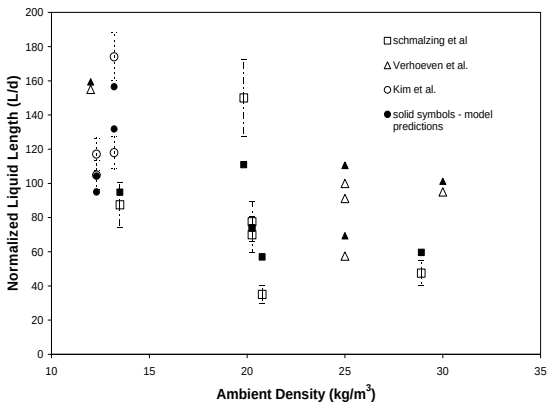


**Figure 2: Comparison of the Liquid Length Model with Dodecane Data from Various Sources.**

**TABLE 1: SURROGATE FUEL PROPERTIES**

| Fuel | Critical Temperature (K) | Critical Pressure (bar) | Boiling Point (K) |
|---|---|---|---|
| dodecane | 658 | 18.2 | 489 |
| tetradecane | 693 | 15.7 | 526 |
| cetane | 723 | 14.0 | 560 |
| heptadecane | 736 | 13.4 | 575 |
| HMN | 692 | 15.7 | 513 |
| DF-2 | NA | NA | 580* |
| JP-8 | NA | NA | 496* |

*90% distillation point

Fuel Enthalpy: The saturated fuel enthalpy was given and based on the reduced saturated temperature as shown below:

$$P_{r,s} < 0.2 \qquad h_f(T_s) = A \bullet T_{r,s} - B$$
$$P_{r,s} \geq 0.2 \qquad h_f(T_s) = -C \bullet T_{r,s}^2 + D \bullet T_{r,s} - E \qquad \textbf{(3)}$$

where A, B, C, D and E are fuel dependent constants given in table 2 while $T_{r,s}$ and $P_{r,s}$ are the reduced saturated temperature and pressure.

**TABLE 2: FUEL ENTHALPY CONSTANTS**

| Fuel | A | B | C | D | E |
|---|---|---|---|---|---|
| dodecane | 1562.5 | 444.84 | 1921.9 | 4996.7 | 1978 |
| tetradecane | 1683.8 | 469.88 | 3712.2 | 8085.6 | 3229.2 |
| cetane | 1869.7 | 550.15 | 929.51 | 3520.3 | 1283.4 |

The injected fuel enthalpy was derived based on the cylinder reduced pressure as given below:

$$\begin{aligned} &\text{dodecane} && h_f(T_f, P_a) = 1.277 \bullet P_{a,r} + 316.3 \\ &\text{tetradecane} && h_f(T_f, P_a) = 1.1718 \bullet P_{a,r} + 319.2 \\ &\text{cetane} && h_f(T_f, P_a) = 1.0429 \bullet P_{a,r} + 320.95 \end{aligned} \quad \textbf{(4)}$$

where $P_{a,r}$ is the reduced ambient pressure and $T_f$ is the liquid fuel temperature.

Fuel Compressibility and Density: The fuel vapor compressibility was determined based on the reduced saturation temperature and its general relationship is given below:

$$Z_f(T_s, P_s) = -a \bullet T_{r,s}^3 + b \bullet T_{r,s}^2 - c \bullet T_{r,s} + d \quad \textbf{(5)}$$

**TABLE 3: FUEL COMPRESSIBILITY CONSTANTS**

| Fuel | A | b | c | d |
|---|---|---|---|---|
| dodecane | 16.85 | 36.104 | 26.425 | 7.5406 |
| tetradecane | 17.924 | 36.143 | 24.71 | 6.6857 |
| cetane | 16.587 | 34.594 | 24.531 | 6.869 |

Furthermore, fuel liquid fuel density is given according to the following compressibility correction relationship:

$$\frac{1}{\rho_s} = \left( \frac{R \bullet T_c}{P_c} \right) \bullet Z_{ra}^{\left\{ 1+(1-T_{f,r})^{2/7} \right\}} \quad \textbf{(6)}$$

where $T_c$ and $P_c$ are fuel critical temperature and pressure, R is the ideal gas constant, $Z_{ra}$ is the Rackett parameter (dodecane: 0.2471, tetradecane: 0.238, cetane: 0.2386), and $T_{f,r}$ is the reduced liquid fuel temperature.

Fuel Saturation Pressure: This relationship was provided and given below:

$$Ln(P_s) = C1 - \frac{C2}{T_s} - C3 \bullet Ln(T_s) + C4 \bullet T_s^2 + \frac{C5}{T_s^2} \quad \textbf{(7)}$$

**TABLE 4: FUEL SATURATION CONSTANTS**

| Fuel | C1 | C2 | C3 | C4*10$^6$ | C5 |
|---|---|---|---|---|---|
| dodecane | 170.27 | 25990 | 20.822 | 2.9759 | 645190 |
| tetradecane | 130.78 | 20072 | 15.743 | 2.531 | -1008900 |
| cetane | 174.2 | 28534 | 21.09 | 2.5228 | 88111 |

Ambient Enthalpy: Tabulated data for air (Moran and Shapiro, 2000) was curve-fit over multiple temperature ranges in order to reduce associated empirical errors. These relationships are given below:

$$\begin{aligned} &450K < T < 599K && h_a(T_a) = 1.033 \bullet T_a - 13.605 \\ &600K \le T < 799K && h_a(T_a) = 1.0735 \bullet T_a - 37.788 \\ &800K \le T < 999K && h_a(T_a) = 1.1184 \bullet T_a - 73.254 \\ &1000K \le T < 1320K && h_a(T_a) = 1.1682 \bullet T_a - 123.49 \end{aligned} \quad \textbf{(8)}$$

Last, the ambient pressure was determined by the ideal gas law assuming a compressibility of unity which was appropriate for the boundary conditions encountered in this study.

### 1.2 Multi-component Surrogates Benchmark

The proposed strategies for properly assessing multi-component surrogate evaporation rate were based on determining subcomponent mass fractions by a boiling point weighting scheme and then either weighting the individual subcomponent liquid length predictions OR weighting the evaporation coefficient and subsequently determining the resulting liquid length. The former approach is referred to as the Mean Liquid Length (MLL) method while the latter is referred to as the Mean Evaporation Coefficient Method (MEC). Each method is mathematically described below:

$$B_s = \sum_{i=1}^{n} x_i B_i \qquad T_b = \sum_{i=1}^{n} T_{b,i} x_i \qquad \sum_{i=1}^{n} x_i = 1 \quad \textbf{(9)}$$

$$L_b = \sum_{i=1}^{n} x_i L_{b,i} \quad \textbf{(10)}$$

where $B_i$ is the evaporation coefficient of component i, $x_i$ is the mass fraction of component i, $T_b$ is the fuel boiling point, $T_{b,i}$ is the boiling point of component i, and $L_{b,i}$ is the liquid length of component i. Comparison of each method was made with data acquired for HMN and a HMN-cetane blend along with a purely analytical exercise of modeling tetradecane as a dodecane-cetane blend, and the proposed MEC method yielded a more accurate predictive technique versus the MLL method (Espey and Dec, 1995; Siebers, 1999; Schihl et al., 2006).

### 1.3 JP-8 Surrogates

Based on the MEC method through equations (9) and (10) it was determined that one potential JP-8 blend is 18% tetradecane/82% dodecane. Since this blend is predominately dodecane, it is reasonable to also assess the possibility of using a single component surrogate for JP-8 as dependent on the variance between the two possible surrogates. The resulting predictions by each method are shown in figure 3 and highlights that using either dodecane or the MEC method could provide comparable predictive capability.

## 2. IGNITION MODELING

There is little if any published literature on JP-8 ignition behavior at elevated pressures let alone at thermodynamic conditions encountered in a diesel engine. The primary issue with modeling JP-8 ignition is that the cetane number can drastically vary depending on the supply source since JP-8 does not have a cetane number specification (MIL-DTL-83133). Continental United

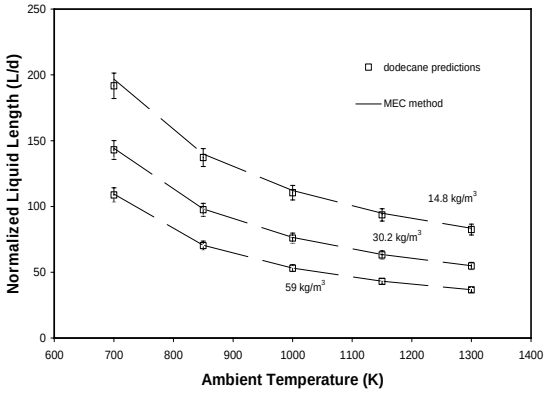


**Figure 3: Comparison of Possible JP-8 Surrogates at Various Ambient Temperatures and Densities.**

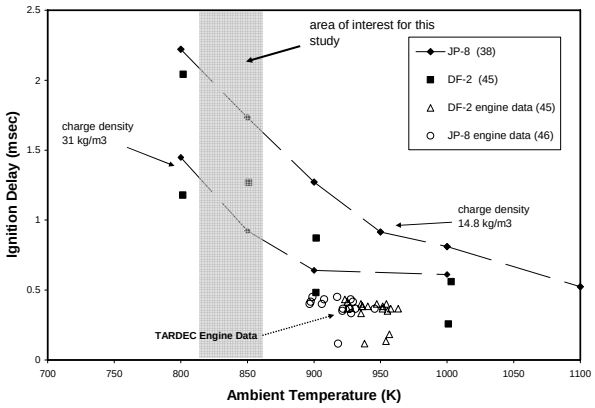


**Figure 4: Comparison of DF-2 and JP-8 Ignition Data at Various Ambient (Charge) Densities. The 30% line represents a 30% increase above the DF-2 data; cetane number for each fuel is given in parenthesis within the legend.**

States (CONUS) procurement data collected by Defense Energy Support Center in 2004 accentuates this issue where the indirectly measured cetane index ranged from 29 to 51 with a mean of 43.9 and a variance of 13.69 (Muzzell et al., 2006). Though cetane index is a not a precise indicator of ignition quality it still provides a sense of cetane number variability in CONUS. Therefore published data on DF-2 that covers a variance of cetane numbers was used to extrapolate the ignition delay period associated with using JP-8 in a diesel engine. Such data revealed that an average 30% increase in the ignition delay period would occur for a decrease of ten in the cetane number (Shipinski et al., 1970; Hardenburg and Hase, 1979; McMillan et al., 1983; Xia and Flanagan, 1987; Teng et al., 2003) assuming that kinetics dominates the ignition delay processes. Recent limited unpublished data from a constant volume bomb substantiated the 30% reduction over an ignition temperature and charge density range included in this study (private communication with Sandia National Laboratory) – see figure 4. Additionally, engine data from a high output single cylinder diesel also further substantiated the assumption that cetane number tends to dominate the ignition delay period when comparing DF-2 and JP-8 as shown in figure 4 where each fuel type had comparable cetane indices.

## 3. ENGINE PREDICTIONS

The Hercules Recovery Vehicle (HRV) diesel engine was chosen for this study since it had exhibited a potential fuel effects combustion issue that could result in eventual engine failure and analog in-cylinder pressure data was available through the engine manufacturer thus allowing more readily for combustion system spray analysis.

**TABLE 5: TELEDYNE CONTINENTAL MOTORS (TCM) AVDS-1790 ENGINE SPECIFICATIONS**

| Engine Parameter | **Description** |
|---|---|
| Number of Cylinders | 12 |
| Bore x stroke (mm) | 146.1 x 146.1 |
| Displacement per cylinder (cc) | 2447 |
| Compression Ratio | 14.5 |
| Rated Speed (rpm) | 2400 |
| Maximum Power (kW) | 780 |
| Peak Injection Pressure (bar) | 650 |
| Nozzle Geometry (mm) | 10 x 0.282 |

The combustion chamber is an off-set bowl with valve cut-outs and a ‘pent roof’ head that is non-ideal for controlling outward squish flow thus increasing the probability for spray-liner interaction. This engine is capable of operating on DF-2 and JP-8 through a mechanical adjustment to the fuel pump that ensures similar fuel mass delivery rate. Nevertheless, in CONUS there have been a number of reports concerning excessive piston erosion problems while operating on JP-8 that suggests a potential combustion system issue revolving around spray targeting. To address this issue, an engine was instrumented with typical performance and combustion measurements and run on both DF-2 and CONUS JP-8. The former had a cetane number of approximately 45 while the latter was 49 which is high in comparison to CONUS JP-8 procurement data discussed in section 2. This experiment yielded no evidence of erosion so a comprehensive spray study was undertaken to extrapolate the combustion system behavior for a JP-8 with a CONUS representative cetane number of near 40. Data taken from the engine experiments was employed to provide boundary conditions for both engine cycle and spray simulations to assess potential spray targeting and related rate of pressure rise issues.

### 3.1 Evaporation Analysis

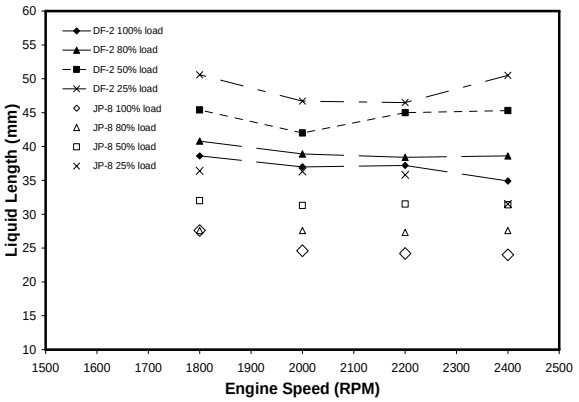


**Figure 5: Comparison of DF-2 and JP-8 Liquid Lengths in the TCM 1790 at Various Operating Conditions.**

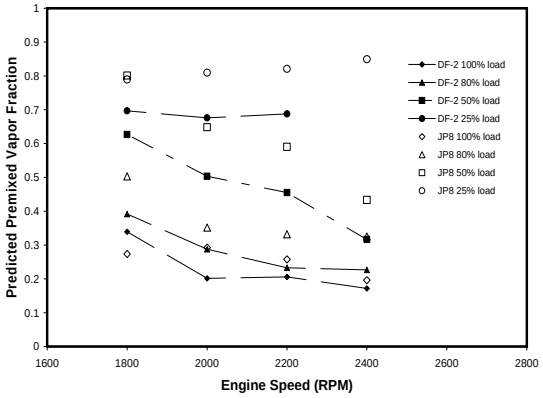


**Figure 6: Comparison of JP-8 and DF-2 Premixed Phase Fuel Vapor Fraction in the TCM 1790 at Various Operating Conditions**

Knowledge of the evaporation rate and the combustible fuel vapor fraction at ignition is necessary in order to assess the initial burn rate in a diesel engine and subsequent rate of pressure rise rate. Predicting the liquid length, i.e. evaporation rate, requires initial combustion chamber thermodynamic conditions such as temperature and density that were not readily available through the aforementioned engine experiments. Therefore, an engine cycle simulation model was built (GT-Power, 2004) and calibrated over the engine's full load operating curve to match measured air flow, manifold pressure, and peak cylinder pressure data. The resulting engine model was employed to provide the aforementioned cylinder thermodynamic conditions for predicting liquid length, spray penetration, and cylinder pressure rise rate.

The predicted liquid lengths for both DF-2 and JP-8 as related to engine speed and load are shown in figure 5. This analysis shows that the JP-8 liquid length is 30% to 40% shorter than DF-2 which is not a surprise considering the 80K difference in the 90% distillation point. Next, the fuel vapor fraction at ignition maybe calculating assuming a 30% increase in ignition delay for the lower cetane number JP-8 as discussed in section 2 assuming that the liquid is a contiguous solid pipe and the mean injection rate maybe used to determine the injected fuel mass upon ignition. Therefore, the evaporated fuel is modeled with the following relationship:

$$m_{evap} = \int_{t_{SOI}}^{t_{IGN}} \dot{m}_{inj}\, dt - \pi \bullet \frac{d^2}{4} \bullet L_b \qquad \textbf{(11)}$$

and $\dot{m}_{inj}$ is the injection rate, $t_{soi}$ is start of injection time, and $t_{ign}$ is the start of ignition. The predicted vapor fraction at ignition reveals (see figure 6) that JP-8 is 15% to 30% higher in comparison to DF-2 and thus it is anticipated that JP-8 would yield both higher premixed phase heat release and pressure rise rate.

### 3.2 Combustion Analysis

To assess the pressure rise rate, a first law analysis was performed on the combustion chamber at the ignition point under the assumption of negligible blow-by effects, i.e. nil mass escaping into the crankcase. The resulting expression is given below:

$$\frac{dP}{dt} \approx \frac{k-1}{V}\left[ \dot{m}_b\, LHV - \frac{dV}{dt} P \bullet \left(1 + \frac{1}{k-1}\right) - \dot{Q}_{wall} \right] \qquad \textbf{(12)}$$

where P is the bulk cylinder pressure, V is the cylinder volume, $\dot{m}_b$ is the fuel burning rate, LHV is the fuel lower heating value, k is the specific heat ratio, and $\dot{Q}_{wall}$ is the heat transfer to the combustion chamber surfaces. For standard diesel combustion the heat transfer term is generally small in comparison to the expansion and combustion terms during the autoignition period since bulk temperatures are relatively low in comparison to later in the compression/expansion strokes. The combustion term tends to dominate during this event in comparison to the expansion term though the later is not entirely negligible and can contribute up to 20% in the predicted pressure rise rate under certain engine operating conditions (Schihl et al., 2006).

The peak pressure rise rate is dictated by the peak fuel burning rate or the point where the premixed phase of heat release reaches a maximum in standard diesel combustion regimes of operation. (Standard diesel combustion is defined as a two phase event comprised of premixed and mixing controlled phases.) During the premixed phase of combustion a premixed turbulent mixing layer that encompasses the fuel jet ignites in multiple locations and correspondingly, turbulent

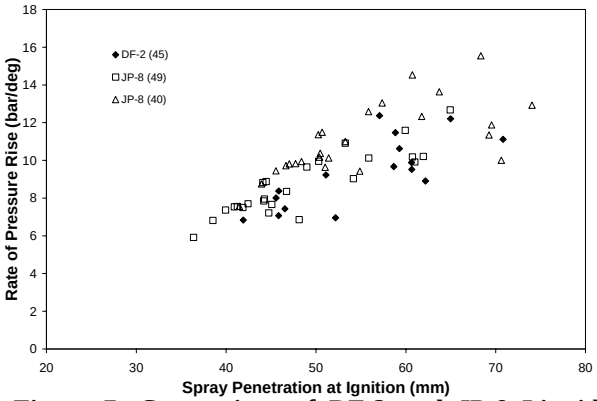


**Figure 7: Comparison of DF-2 and JP-8 Liquid Lengths in the TCM 1790 at Various Operating Conditions. The cetane number for each fuel is given in the legend.**

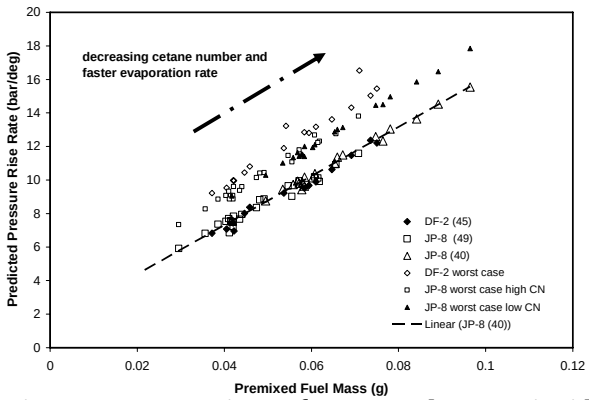


**Figure 8: Comparison of DF-2 and JP-8 Liquid Lengths in the TCM 1790 at Various Operating Conditions. The cetane number for each fuel is given in the legend.**

flamelets are generated and propagate rapidly throughout the shear layer. This event normally takes place within a few crank angles or tenths of a millisecond in a diesel engine due to the high turbulent entrainment and subsequent burning rates associated with high pressure diesel jets. Based on extensive experience with other diesel engines, the TARDEC Large Scale Combustion Model (LSCM) was employed to predict the maximum fuel burning rate based on the 'flamelet in eddies' assumption (Turns, 1996; Schihl et al., 1999). Essentially, this peak occurs when the shear layer is completely engulfed in a turbulent flame and represents approximately the consumption of one-half of the trapped shear layer fuel mass.

The resulting predicted pressure rise rates for the both JP-8 and DF-2 are shown in figure 7 as a function of spray tip penetration as determined by a well known two zone model (Hiroyasu and Arai, 1990). Qualitatively this trend makes sense since longer spray penetration correlates to a large premixed fuel vapor fraction given that longer ignition times allow for more thorough mixing. Thus, a more fundamental portrayal of this event is given in figure 8 that highlights the direct correlation between the cylinder pressure rise rate and the vapor mass trapped in the shear layer at ignition based on the aforementioned 'flamelet in eddies' approach (Turns, 1996; Schihl et al., 1999) that tends to exhibit a relatively constant combustion timescale.

Nevertheless, this trend is important when comparing the overall combustion characteristics of operating the TCM 1790 on DF-2 versus JP-8 especially considering the aforementioned piston erosion problems exhibited in CONUS operation. For a given fuel, a decrease in the cetane number increases the premixed fuel mass causing an increase in pressure rise rate which is further augmented by fuels with higher volatility that again tend to increase the premixed fuel mass. This study has only included predictions for JP-8 with a cetane number near 40 even though aforementioned CONUS data (see section 2) has revealed cetane indices approaching 29. Thus, it is anticipated that the pressure rise rate would substantially increase for such a low ignition quality fuel in comparison to the 40 cetane number JP-8 included in this study. Such behavior is important since diesel engines have a design pressure rise rate and peak cylinder pressure limit that if exceeded will lead to eventual propulsion system failure. These predictions are conservative since it is known that mixing occurs after ignition and that the effective premixed fuel mass fraction increases during the ignition delay period. In order to address this situation a worst case scenario is also included in figure 8 that includes the assumption that all fuel injected during the ignition delay period atomizes, evaporates, and mixes fast enough to be consumed during the premixed phase of the heat release event. In general, this worst case scenario lent toward a 20% or higher pressure rise rate in comparison to the aforementioned more conservative approach.

Based on the aforementioned analysis a number of suggestions were made to the engine manufacturer, vehicle manufacturer, and PM Hercules for remedying the piston erosion issue. First, redesign the piston bowl to control spray over-penetration by increasing the diameter and modifying the bowl entry angle. Second, reduce the injector nozzle hole sizes to control spray over-penetration. Third, consider using a high pressure common rail fuel system in parallel with suggestion two for both controlling over-penetration and improving power density. Last, redesign the intake manifolds to allow for less variability in cylinder-to-cylinder air-fuel ratio and thus reduce ignition variability among cylinders.

## CONCLUSION

A method for assessing potential combustion characteristic differences for JP-8 versus DF-2 has been developed and applied to a military diesel engine that was

experiencing piston erosion issues. In particular, a multi-component evaporation methodology was developed based on past work by other engine researchers that resulted in the development of a JP-8 evaporation surrogate. Furthermore, ignition data collected through bomb and engine experiments validated the JP-8 ignition assumption that conservatively, a ten cetane number decrease correlates to a 30% increase in the ignition delay period – this is the first known JP-8 ignition data set at diesel engine boundary conditions. Last, a scaling method was developed to correlate pressure rise rate with shear layer fuel mass through judicious scaling of the evaporation rate, injection timing, and ignition timing events. Collectively, these new findings will help address potential fuel related combustion issues with current vehicles as presented in this submission and also aide in the development of future military diesel engines.

## ACKNOWLEDGEMENTS

The authors wish to thank the TARDEC propulsion laboratory, L3COM, and PM Hercules for their support.

## REFERENCES

American Petroleum Institute, 1997, **Technical Data Book Petroleum Refining**, 6th Edition.

Bower, G.R. and Foster, D.E., 1993, "The Effect of Split Injection on Fuel Distribution in an Engine-Fed Combustion Chamber", SAE Paper 930864.

Cernansky, N., 2006, "Low Temperature Oxidation Chemistry of JP-8", ARO-AFSOR Contractors Meeting.

Espey, C. and Dec, J., 1995, "The Effect of TDC Temperature and Density on the Liquid-Phase Fuel Penetration in a D.I. Diesel Engine", SAE Paper 952456.

GT-Power User's Manual, 2004, GT-Suite™ Version 6.1, Gamma Technologies.

Hanson, R.K., 2006, "Laser Diagnostics for Reacting Flows", ARO-AFSOR Contractors Meeting.

Hardenburg, H.O. and Hase, F.W., 1979, "An Empirical Formula for Computing the Pressure Rise Delay of a Fuel from its Cetane Number and from Relevant Parameters of Direct-Injection Diesel Engines", SAE Paper 790493.

Hiroyasu, H. and Arai, M., "Structure of Fuel Sprays in Diesel Engines", SAE Paper 900475, 1990.

Hodges, J.T., Baritaud, T.A., and Heinze, T.A., 1991, "Planar Liquid and Gas Fuel and Droplet Size Visualization in a DI Diesel Engine", SAE Paper 910726.

Kim, T., Beckman, M.S., Farrell, P.V., and Ghandhi, J.B., 2002, "Evaporating Spray Concentration Measurements from Small and Medium Bore Diesel Injectors", SAE Paper 2002-01-00219.

McMillan, M.L., Siegla, D.C., Srinivasan, N., and Tuteja, A.D., 1983, "A Review of GM Investigations of the Effects of Fuel Characteristics on Diesel Engine Combustion and Emissions", Coordinating Research Council Diesel Fuel Workshop.

Metghalchi, M., 2006, "Autoignition and Burn Speeds of Liquid Fuels", ARO-AFOSR Contractors Meeting.

Miklos, A., 1989, "JP-8/Jet A Fuel Qualification Test in Engines Representative of the U.S. Army Stock", U.S. Army Tank-Automotive RD&E Center Report 13473.

Moran, M.J. and Shapiro, H.N., **2000, Fundamentals of Engineering Thermodynamics,** John Wiley & Sons.

Muzzell, P.A., Sattler, E.R., Terry, A., McKay, B.J., Freerks, R.L., Stavinoha, L.L., 2006, "Properties of Fischer-Tropsch (FT) Blends for Use in Military Equipment", SAE Paper 2006-01-0702.

Schihl, P., Hoogterp, L., and Pangilinan, H., 2006, "Assessment of JP-8 and DF-2 Evaporation Rate and Cetane Number Differences on a Military Diesel Engine", SAE Paper 2006-01-1549.

Schihl, P.J., Atreya, A., Bryzik, W., and Schwarz, E., 1999, "Simulation of Combustion in Direct-Injection Low Swirl Heavy-Duty Type Diesel Engines", SAE Paper 1999-01-0228.

Schmalzing, C.-O., Stapf, P., Maly, R.R., Stetter, H., and Dwyer, H.A., 1999, "A Holistic Hydraulic and Spray Model – Liquid and Vapor Phase Penetration of Fuel Sprays and DI Diesel Engines", SAE Paper 1999-01-3549.

Shipinski, J., Myers, P.S., and Uyehara, O.A., 1969-70, "A Spray Droplet Model for Diesel Combustion", *Symposium on Diesel Engine Combustion*, Institution of Mechanical Engineers, **184**, 28 - 35.

Siebers, D., 1999, "Scaling Liquid-Phase Penetration in Diesel Sprays Based on Mixing-Limited Vaporization", SAE Paper 1999-01-0528.

Siebers, D.L., 1998, Liquid-Phase Fuel Penetration in Diesel Sprays", SAE Paper 980809.

Teng, H., McCandless, J.C., and Schneyer, J.B., 2003, "Compression Ignition Delay of Dimethyl Ether – An Alternative Fuel for Compression-Ignition Engines", SAE Paper 2003-01-0759.

Turns, S., 1996, **An Introduction to Combustion: Concepts and Applications**, McGraw-Hill Inc.

Verhoeven, D., Vanhemelryck, J. –L., and Baritaud, T., 1998, "Macroscopic and Ignition Characteristics of High-Pressure Spays and Single-Component Fuels", SAE Paper 981069.

Xia, Y.Q. and Flanagan, R.C., 1987, "Ignition Delay – A General Engine/Fuel Model", SAE Paper 870591.

Yeh, C.-N., Kanimoto, T., Kobori, S., and Kosaka, H., 1993, "2-D Imaging of Fuel Vaport Concentration in a Diesel Spray via Exciplex-Based Fluorescence Technique", SAE Paper 932652.